Acta Mech Sinica (2006) 22: 170–176
DOI 10.1007/s10409-005-0093-z

RESEARCH PAPER

Zhi Han · Haitian Yang · Ling Liu

Solving viscoelastic problems with cyclic symmetry via a precise algorithm and EFGM*

Received: 17 January 2005 / Accepted: 2 November 2005 / Revised: 23 November 2005 / Published online: 14 March 2006

Abstract The paper combines a self-adaptive precise algorithm in the time domain with Meshless Element Free Galerkin Method (EFGM) for solving viscoelastic problems with rotationally periodic symmetry. By expanding variables at a discretized time interval, the variations of variables can be described more precisely, and iteration is not required for non-linear cases. A space-time domain coupled problem with initial and boundary values can be converted into a series of linear recursive boundary value problems, which are solved by a group theory based on EFGM. It has been proved that the coefficient matrix of the global EFG equation for a rotationally periodic system is block-circulant so long as a kind of symmetry-adapted reference coordinate system is adopted, and then a partitioning algorithm for facilitating parallel processing was proposed via a completely orthogonal group transformation. Therefore instead of solving the original system, only a series of independent small sub-problems need to be solved, leading to computational convenience and a higher computing efficiency. Numerical examples are given to illustrate the full advantages of the proposed algorithm.

Keywords EFGM · Cyclic symmetry · Precise algorithm · Viscoelastic problem

1 Introduction

Viscoelasticity is related to many engineering applications. The activities in this field have been primarily due to the large scale development and utilization of polymeric materials [1]. Viscoelastic problems are time dependent. Due to complex material properties, boundary conditions, and boundary shapes etc., analytical solutions are hardly obtained in general. A variety of step-by-step based numerical techniques have been developed. The assumptions [2–4] that variables remain constant or change linearly at a discretized time interval were conventionally adopted. The adaptability of computing accuracy to the change of sizes of time steps [5], which is generally difficult to be predicted in the computation, seems not to be much concerned with. In addition to the computing accuracy, computing expense in each time step is a decisive factor affecting the whole computing efficiency.

With the above consideration, a self-adaptive precise algorithm which was previously used for the solution of differential equation system only [5–8] is further developed in the present paper. By expending all variables at two levels at a discretized time interval, a differential-integral equation system with boundary and initial values is converted into a series of linear recurrent boundary value problems which are solved via Element-Free Galerkin Method (EFGM). In the procedure of solving recursive EFG equations, adaptive computation can be carried out with different sizes of time steps.

EFGM is a promising method which does not require any element connectivity data and does not suffer much degradation in accuracy when nodal arrangements are very irregular [9]. However higher computing expense, by comparison with FEM etc., is one of the obstacles to limit its application. In this paper, for a special kind of viscoelastic structure, i.e. the structure with cyclic symmetry which was much exploited in the structural FE and BE analysis [10–15], an effort has been made to make up such deficiency by utilizing the cyclic symmetry via a partitioning algorithm.

The benefits obtained by combining self-adaptive precise and partitioning algorithms are two folds. (1) In the time domain a self-adaptive computation can result in a more precise description for the variation of variables and compensating any possible loss of computing accuracy caused by improper choices of the size of time step. For non-linear

*The project supported by the National Natural Science Foundation of China ((10421002, 10472019 and 10172024); NKBRSF (2005CB321704) and the Fund of Disciplines Leaders of Young and Middle Age Faculty in Colleges of Liaoning Province. The English text was polished by Yunming Chen.

Z. Han · H. T. Yang (✉) · L. Liu
State Key Lab of Structural Analysis of Industrial Equipment,
Department of Engineering Mechanics,
Dalian University of Technology,
Dalian 116024, China
E-mail: haitian@dlut.edu.cn
Tel.:+86-411-84708394

cases, no assumption is made and no iteration is needed. (2). In the space domain, only series of small subproblems are required to be solved independently instead of the whole EFG equations. Thus the computational efficiency is significantly increased.

The computational convenience and efficiency of presented approach are fully discussed and demonstrated by means of numerical examples.

2 Recurrent governing equations

The governing equations of viscoelasticity can be described by [16]

$$\boldsymbol{H}\boldsymbol{\sigma} + \boldsymbol{b} = 0, \tag{1}$$

$$\boldsymbol{\varepsilon} = \boldsymbol{H}^{\mathrm{T}}\boldsymbol{u}. \tag{2}$$

The boundary conditions are specified by [16]

$$\boldsymbol{u} = \tilde{\boldsymbol{u}} \qquad x \in \Gamma_u, \tag{3}$$

$$\boldsymbol{P} = \tilde{\boldsymbol{P}} \qquad x \in \Gamma_\sigma, \tag{4}$$

where $\boldsymbol{\sigma}$ and $\boldsymbol{\varepsilon}$ denote the vector of stress and strain, respectively, $\boldsymbol{b}$ is the vector of body force, $\boldsymbol{u}$ is the vector of displacement, $\boldsymbol{P}$ denotes the vector of traction, $\tilde{\boldsymbol{u}}$, $\tilde{\boldsymbol{P}}$ are the prescribed values of $\boldsymbol{u}$ and $\boldsymbol{P}$ on the boundary, respectively.

$$\boldsymbol{H} = \begin{bmatrix} \partial/\partial x & 0 & \partial/\partial y \\ 0 & \partial/\partial y & \partial/\partial x \end{bmatrix}. \tag{5}$$

Divide time domain into a number of time intervals, the initial points and sizes of the time intervals are defined by $\tau_0, t_1, t_2, \ldots, t_k \ldots$ and $T_1, T_2, \ldots, T_k \ldots$, respectively. At a discretized time interval, in order to describe the variation of variables more precisely, all variables are expanded in terms of s

$$\boldsymbol{\sigma} = \sum_{m=0} \boldsymbol{\sigma}^m s^m, \tag{6}$$

$$\boldsymbol{\varepsilon} = \sum_{m=0} \boldsymbol{\varepsilon}^m s^m, \tag{7}$$

$$\boldsymbol{b} = \sum_{m=0} \boldsymbol{b}^m s^m, \tag{8}$$

$$\boldsymbol{u} = \sum_{m=0} \boldsymbol{u}^m s^m, \tag{9}$$

$$\tilde{\boldsymbol{u}} = \sum_{m=0} \tilde{\boldsymbol{u}}^m s^m \tag{10}$$

$$\boldsymbol{P} = \sum_{m=0} \boldsymbol{P}^m s^m, \tag{11}$$

$$\tilde{\boldsymbol{P}} = \sum_{m=0} \tilde{\boldsymbol{P}}^m s^m, \tag{12}$$

$$s = \frac{t - t_{k-1}}{T_k}, \tag{13}$$

where t_{k-1} and T_k represent the initial point and size of the k-th time interval, respectively, $\boldsymbol{\sigma}^m$ and $\boldsymbol{\varepsilon}^m$ represent the expanding coefficients of $\boldsymbol{\sigma}$ and $\boldsymbol{\varepsilon}$, respectively, $\boldsymbol{b}^m$ denotes the expanding coefficient of $\boldsymbol{b}$, $\boldsymbol{u}^m$, $\boldsymbol{P}^m$, $\tilde{\boldsymbol{u}}^m$ and $\tilde{\boldsymbol{P}}^m$ are the expanding coefficients of $\boldsymbol{u}$, $\boldsymbol{P}$, $\tilde{\boldsymbol{u}}$, and $\tilde{\boldsymbol{P}}$, respectively. The conversion relationship between the differentiations respect to t and s is

$$\frac{\mathrm{d}}{\mathrm{d}t} = \frac{1}{T_k}\frac{\mathrm{d}}{\mathrm{d}s}, \tag{14}$$

$$\frac{\mathrm{d}^2}{\mathrm{d}t^2} = \frac{1}{T_k^2}\frac{\mathrm{d}^2}{\mathrm{d}s^2}. \tag{15}$$

Substituting Eqs. (6)–(12) into Eqs. (1)–(4) yields

$$\boldsymbol{H}\boldsymbol{\sigma}^m + \boldsymbol{b}^m = 0, \tag{16}$$

$$\boldsymbol{\varepsilon}^m = \boldsymbol{H}^{\mathrm{T}}\boldsymbol{u}^m, \tag{17}$$

$$\boldsymbol{u}^m = \tilde{\boldsymbol{u}}^m \qquad x \in \Gamma_u, \tag{18}$$

$$\boldsymbol{P}^m = \tilde{\boldsymbol{P}}^m \qquad x \in \Gamma_\sigma. \tag{19}$$

3 Recurrent constitutive equations

A viscoelastic constitutive equation can be written in an integral form [1]

$$\boldsymbol{\varepsilon}(t) = \boldsymbol{D}^{*-1}\left\{\boldsymbol{\sigma}(t)A(t) - \int_{\tau_0}^{t} \boldsymbol{\sigma}(\tau)\frac{\partial}{\partial\tau}[A(\tau) + C(t,\tau)]\mathrm{d}\tau\right\}, \tag{20}$$

where τ_0 is the lower limit of integration, $A(\tau) = \dfrac{1}{E(\tau)}$, $E(t)$ denotes Young's modulus, $C(t,\tau) = \varphi(\tau)\left(1 - \sum_{l=1}^{L} \mathrm{e}^{-\gamma_l(t-\tau)}\right)$, $l = 1, \ldots, L$, $\varphi(\tau) = (a + b/\tau)$, $\varphi(\tau)$ and $C(t,\tau)$ are the known functions, γ, a and b represent material parameters, $\boldsymbol{\varepsilon}(t) = \{\varepsilon_x(t)\ \varepsilon_y(t)\ \gamma_{xy}(t)\}^{\mathrm{T}}$, $\boldsymbol{\sigma}(t) = \{\sigma_x(t)\ \sigma_y(t)\ \tau_{xy}(t)\}^{\mathrm{T}}$. $\boldsymbol{D}^*$ is defined by

$$\boldsymbol{D}^* = \frac{1}{1-\nu^2}\begin{bmatrix} 1 & \nu & 0 \\ \nu & 1 & 0 \\ 0 & 0 & \dfrac{1-\nu}{2} \end{bmatrix}, \tag{21}$$

where ν is the Poisson ratio. By utilizing a two-level expanding technique [17], recursive equations of Eq. (20) can be obtained.

At the first time interval, $t \in [\tau_0, \tau_0 + T_1]$, using the precise algorithm, one has [17]

$$\boldsymbol{D}^*\boldsymbol{\varepsilon}^0 = A^0\boldsymbol{\sigma}^0 \qquad R = 0, \tag{22}$$

$$\boldsymbol{D}^*\boldsymbol{\varepsilon}^R = \sum_{m=0}^{R} A^m\boldsymbol{\sigma}^{R-m} + \boldsymbol{ET}(R) \quad R \neq 0, \tag{23}$$

where

$$\boldsymbol{ET}(R) = -\frac{1}{R}\sum_{m=0}^{R-1}(m+1)A^{m+1}\boldsymbol{\sigma}^{R-m-1} - \frac{1}{R}\sum_{m=0}^{R-1}(m+1)\varphi^{m+1}\boldsymbol{\sigma}^{R-m-1} + \sum_{l=1}^{L}\Big(\sum_{k=0}^{R-1}\frac{1}{k+1}\Big(\sum_{n=0}^{k}(n+1) \times\Big(\sum_{m=0}^{n+1}\varphi^{m}e_{2l}^{n-m+1}\Big)\boldsymbol{\sigma}^{k-n}\Big)e_{1l}^{R-k-1}\Big), \tag{24}$$

$$e^{-T_k\gamma_l s} = \sum_{m=0} e_{1l}^{m}s^{m} = \sum_{m=0}\frac{(-T_k\gamma_l)^m}{m!}s^{m}, \tag{25}$$

$$e^{T_k\gamma_l \xi} = \sum_{m=0} e_{2l}^{m}\xi^{m} = \sum_{m=0}\frac{(T_k\gamma_l)^m}{m!}\xi^{m}. \tag{26}$$

At the other intervals, one has

$$\boldsymbol{D}^{*}\boldsymbol{\varepsilon}^{R} = \sum_{m=0}^{R}A^{m}\boldsymbol{\sigma}^{R-m} + \boldsymbol{EPT}(R) \quad R\neq 0, \tag{27}$$

$$\boldsymbol{EPT}(R) = \sum_{l=1}^{L}(e^{-\gamma_l t_k}\boldsymbol{G}_l e_{1l}^{R}) + \boldsymbol{ET}(R), \tag{28}$$

$$\boldsymbol{G}_l = \int_{\tau_0}^{t_{k-1}}\boldsymbol{\sigma}(\tau)\frac{\partial}{\partial\tau}[\varphi(\tau)e^{\gamma_l\tau}]\mathrm{d}\tau. \tag{29}$$

4 Recursive EFG equations

For Eqs.(16)–(19), EFG equations can be expressed as [18],

$$\begin{bmatrix}\boldsymbol{K} & \boldsymbol{G}\\ \boldsymbol{G}^{\mathrm{T}} & \boldsymbol{0}\end{bmatrix}\begin{Bmatrix}\boldsymbol{u}^{R}\\ \boldsymbol{\lambda}^{R}\end{Bmatrix} = \begin{Bmatrix}\boldsymbol{f}^{R}\\ \boldsymbol{q}^{R}\end{Bmatrix} \quad R = 0, 1, 2, \cdots, \tag{30}$$

where $\boldsymbol{K}$ and $\boldsymbol{G}$ are the global coefficient matrices, $\boldsymbol{u}^{R}$ represents the expanding coefficient of $\boldsymbol{u} = \sum \boldsymbol{u}^{R}s^{R}$, $\boldsymbol{\lambda}^{R}$ is the expanding coefficients of vector of Lagrange multiplier $\boldsymbol{\lambda} = \sum \boldsymbol{\lambda}^{R}s^{R}$, $\boldsymbol{u}$ is the vector of parameters employed to represent the displacement $\boldsymbol{u}(\boldsymbol{x})$, and $\boldsymbol{u}^{R}$ can be expressed in the following form by utilizing the moving least square (MLS) method [18]:

$$\boldsymbol{u}^{R}(\boldsymbol{x}) = \sum_{I=1}^{n}\boldsymbol{\Phi}_I(\boldsymbol{x})\boldsymbol{u}_I = \boldsymbol{\Phi}(\boldsymbol{x})\boldsymbol{u}^{R}, \tag{31}$$

where $\boldsymbol{\Phi}_I$ represents a shape function, $\boldsymbol{\Phi}$ is a matrix of shape functions.

$$\boldsymbol{G}_{IK} = -\int_{\Gamma_u}\boldsymbol{\Phi}_I\boldsymbol{N}_K\mathrm{d}\Gamma, \tag{32}$$

$$\boldsymbol{K}_{IJ} = \iint_{\Omega}\boldsymbol{B}_I^{\mathrm{T}}\boldsymbol{D}\boldsymbol{B}_J\mathrm{d}\Omega, \tag{33}$$

$$\boldsymbol{B}_I = \begin{bmatrix}\Phi_{I,x} & 0\\ 0 & \Phi_{I,y}\\ \Phi_{I,y} & \Phi_{I,x}\end{bmatrix}, \tag{34}$$

$$\boldsymbol{N}_k(\boldsymbol{x}) = \begin{bmatrix}N_k(\boldsymbol{x}) & 0\\ 0 & N_k(\boldsymbol{x})\end{bmatrix}, \tag{35}$$

$$\boldsymbol{q}^{R} = -\int_{\Gamma_1}\boldsymbol{N}\tilde{\boldsymbol{u}}^{R}\mathrm{d}\Gamma, \tag{36}$$

$$\boldsymbol{D} = \boldsymbol{D}^{*}/A^{0}$$

for plane stress problems, $\quad R = 0, 1, 2, \ldots,$ (37)

where Γ_u denotes the essential boundary, $N_k(\boldsymbol{x})$ represents a shape function. At the first time interval

$$\boldsymbol{f}_I^{R} = \int_{\Gamma_\sigma}\boldsymbol{\Phi}_I\tilde{\boldsymbol{P}}^{R}\mathrm{d}\Gamma + \int_{\Omega}\boldsymbol{\Phi}_I\boldsymbol{b}^{R}\mathrm{d}\Omega + \int_{\Omega}\boldsymbol{B}_I^{\mathrm{T}}\boldsymbol{ET}(R)/A^{0}\mathrm{d}\Omega. \tag{38}$$

At the other time intervals

$$\boldsymbol{f}_I^{R} = \int_{\Gamma_\sigma}\boldsymbol{\Phi}_I\tilde{\boldsymbol{P}}^{R}\mathrm{d}\Gamma + \int_{\Omega}\boldsymbol{\Phi}_I\boldsymbol{b}^{R}\mathrm{d}\Omega + \int_{\Omega}\boldsymbol{B}_I^{\mathrm{T}}\boldsymbol{EPT}(R)/A^{0}\mathrm{d}\Omega. \tag{39}$$

A self-adaptive computation is carried out at each of the time intervals with a convergence criterion

$$\mathrm{Abs}\Big(\Big(u_k^{R}s^{R}\Big/\sum_{j=0}^{R-1}u_k^{j}s^{j}\Big)_{s=1}\Big) \leq \beta, \tag{40}$$

where β is an error bound, u_k^{j} denotes the k-th component of $\boldsymbol{u}^{j}$ $(j = 1, 2, \ldots, R)$. Every $\boldsymbol{u}^{R}(R = 1, 2, \cdots)$ is required to be checked with the above criterion, if the criterion is satisfied consecutively 3 times, computing will stop at the time interval considered, and step into the next one. If the criterion is not met, the next order $(R+1)$ computation will continue till reaching the convergence.

In the computation, mm, an upper bound of R, will be prescribed in advance. If computing can not stop when $R = mm$, it is necessary to reduce the size of the time step or increase the value of mm, if condition (40) is satisfied when $R \ll mm$, a bigger size of time step can be considered.

5 Rotationally periodic symmetry

A structure or a computational region Ω is said to possess rotationally periodic symmetry of order N when its geometry and physical properties and constraint conditions are invariant under the following N symmetry transformations [13]

$$\Psi_i = (i-1)\theta, \qquad i = 1, 2, \ldots, N, \tag{41}$$

where Ψ_i represents a rotation of Ω about its axis of rotation, $\theta = 2\pi/N$, N is defined as the order of symmetry.

It is convenient that the axis of rotation is defined as the Z-axis in a rectangular or cylindrical coordinate system. Figure 1 shows a plane region possessing rotationally periodic symmetry with $N = 6$.

It is obvious that Ω can be naturally divided into N identical parts. Arranging these N parts in an anti-clock wise sequence, and designating them as $\Omega_i (i = 1, \ldots, N)$, we have

$$\Omega = \Omega_1 \cup \Omega_2 \cup \cdots \cup \Omega_N, \quad \Omega_i = \Psi_i : \Omega_1 \tag{42}$$

Equation (42) means that Ω_i can be obtained from Ω_1, which is called "basic region" and can be arbitrarily chosen from these identical parts. When the EFGM is employed to analyze a rotationally periodic system Ω, to make full use of its symmetry, the background cells, nodes and discrete points along essential boundaries are required to be arranged in a symmetric way, so that all nodes and integration points keeps the original symmetry of the system. Setting up nodal coordinates and integral cells on Ω_1 only, one can then obtain a computational model by using Eq. (42). Provided the numbers of nodes belonging to Ω_1 and discrete points along Γ_1 are denoted as m and n, respectively, then the total computational nodes and discrete points will be Nm and Nn.

6 The properties of global EFG coefficient matricices

In a rotationally periodic system, $\boldsymbol{u}^R$ and $\boldsymbol{\lambda}^R$ in Eq. (30) can be described by [13]

$$\begin{aligned} \boldsymbol{u}^{RT} &= \{\boldsymbol{u}^{1RT}, \boldsymbol{u}^{2RT}, \ldots, \boldsymbol{u}^{NRT}\}, \\ \boldsymbol{\lambda}^{RT} &= \{\boldsymbol{\lambda}^{1RT}, \boldsymbol{\lambda}^{2RT}, \ldots, \boldsymbol{\lambda}^{NRT}\}, \end{aligned} \tag{43}$$

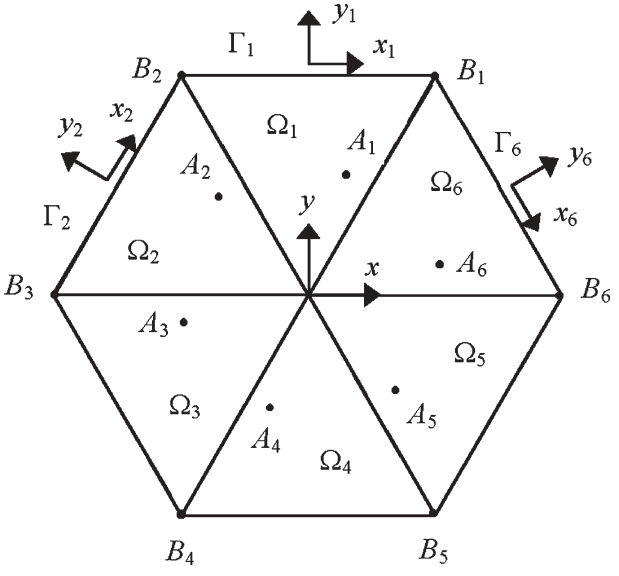

Fig. 1 A rotationally periodic planar plate with $N = 6$

where $\boldsymbol{u}_i^R$ and $\boldsymbol{\lambda}_i^R$, belonging to the i-th symmetry region, are sub-vectors of $\boldsymbol{u}^R$ and $\boldsymbol{\lambda}^R$ with orders $2m$ and $2n$, respectively, and the superscript T denotes the transpose.

In such an ordering way, $\boldsymbol{K}$ and $\boldsymbol{G}$ can be written as

$$\boldsymbol{K} = \begin{bmatrix} \boldsymbol{K}^{11} & \boldsymbol{K}^{12} & \cdots & \boldsymbol{K}^{1N} \\ \boldsymbol{K}^{21} & \boldsymbol{K}^{22} & \cdots & \boldsymbol{K}^{2N} \\ \vdots & \vdots & \ddots & \vdots \\ \boldsymbol{K}^{N1} & \boldsymbol{K}^{N2} & \cdots & \boldsymbol{K}^{NN} \end{bmatrix},$$

$$\boldsymbol{K}^{ij} = \begin{bmatrix} \boldsymbol{K}_{11}^{ij} & \boldsymbol{K}_{12}^{ij} & \cdots & \boldsymbol{K}_{1m}^{ij} \\ \boldsymbol{K}_{21}^{ij} & \boldsymbol{K}_{22}^{ij} & \cdots & \boldsymbol{K}_{2m}^{ij} \\ \vdots & \vdots & \ddots & \vdots \\ \boldsymbol{K}_{m1}^{ij} & \boldsymbol{K}_{m2}^{ij} & \cdots & \boldsymbol{K}_{mm}^{ij} \end{bmatrix}, \tag{44}$$

$$i, j = 1, 2, \cdots, N,$$

$$\boldsymbol{G} = \begin{bmatrix} \boldsymbol{G}^{11} & \boldsymbol{G}^{12} & \cdots & \boldsymbol{G}^{1N} \\ \boldsymbol{G}^{21} & \boldsymbol{G}^{22} & \cdots & \boldsymbol{G}^{2N} \\ \vdots & \vdots & \ddots & \vdots \\ \boldsymbol{G}^{N1} & \boldsymbol{G}^{N2} & \cdots & \boldsymbol{G}^{NN} \end{bmatrix},$$

$$\boldsymbol{G}^{ij} = \begin{bmatrix} \boldsymbol{G}_{11}^{ij} & \boldsymbol{G}_{12}^{ij} & \cdots & \boldsymbol{G}_{1n}^{ij} \\ \boldsymbol{G}_{21}^{ij} & \boldsymbol{G}_{22}^{ij} & \cdots & \boldsymbol{G}_{2n}^{ij} \\ \vdots & \vdots & \ddots & \vdots \\ \boldsymbol{G}_{m1}^{ij} & \boldsymbol{G}_{m2}^{ij} & \cdots & \boldsymbol{G}_{mn}^{ij} \end{bmatrix}, \tag{45}$$

$$i, j = 1, 2, \cdots, N.$$

In a symmetry-adapted systems [12], one has

$$\begin{aligned} \boldsymbol{u}^R &= \boldsymbol{T}^m \cdot \bar{\boldsymbol{u}}^R, \quad \boldsymbol{f} = \boldsymbol{T}^m \cdot \bar{\boldsymbol{f}}, \\ \boldsymbol{\lambda}^R &= \boldsymbol{T}^n \cdot \bar{\boldsymbol{\lambda}}^R, \quad \boldsymbol{q} = \boldsymbol{T}^n \cdot \bar{\boldsymbol{q}}, \end{aligned} \tag{46}$$

$$\boldsymbol{T}^m = \begin{bmatrix} \bar{\boldsymbol{T}}_1^m & & & \boldsymbol{0} \\ & \bar{\boldsymbol{T}}_2^m & \ddots & \\ \boldsymbol{0} & & & \bar{\boldsymbol{T}}_N^m \end{bmatrix},$$

$$\bar{\boldsymbol{T}}_i^m = \begin{bmatrix} \bar{\boldsymbol{T}}_i & & & \\ & \bar{\boldsymbol{T}}_i & & \\ & & \ddots & \\ & & & \bar{\boldsymbol{T}}_i \end{bmatrix}_{2m \times 2m}, \tag{47}$$

$$\boldsymbol{T}^n = \begin{bmatrix} \bar{\boldsymbol{T}}_1^n & & & \boldsymbol{0} \\ & \bar{\boldsymbol{T}}_2^n & & \\ & & \ddots & \\ \boldsymbol{0} & & & \bar{\boldsymbol{T}}_N^n, \end{bmatrix},$$

$$\bar{\boldsymbol{T}}_i^n = \begin{bmatrix} \boldsymbol{T}_i & & & \\ & \boldsymbol{T}_i & & \\ & & \ddots & \\ & & & \boldsymbol{T}_i \end{bmatrix}_{2n \times 2n}, \tag{48}$$

$$\boldsymbol{T}_i = \begin{bmatrix} \cos(i-1)\theta & -\sin(i-1)\theta \\ \sin(i-1)\theta & \cos(i-1)\theta \end{bmatrix}, \theta = 2\pi/N. \quad (49)$$

Substituting Eqs. (47)–(48) into Eq. (30), yields

$$\boldsymbol{K}\boldsymbol{T}^m\bar{\boldsymbol{u}}^R + \boldsymbol{G}\boldsymbol{T}^n\bar{\boldsymbol{\lambda}}^R = \boldsymbol{T}^m\bar{\boldsymbol{f}}^R, \quad (50)$$

$$\boldsymbol{G}^{\mathrm{T}}\boldsymbol{T}^m\bar{\boldsymbol{u}}^R = \boldsymbol{T}^n\bar{\boldsymbol{q}}^R. \quad (51)$$

Multiplying Eqs.(50)–(51) by $\boldsymbol{T}^{m\mathrm{T}}$ and $\boldsymbol{T}^{n\mathrm{T}}$, respectively, then we get

$$\begin{bmatrix} \bar{\boldsymbol{K}} & \bar{\boldsymbol{G}} \\ \bar{\boldsymbol{G}}^{\mathrm{T}} & \boldsymbol{0} \end{bmatrix} \begin{Bmatrix} \bar{\boldsymbol{u}}^R \\ \bar{\boldsymbol{\lambda}}^R \end{Bmatrix} = \begin{Bmatrix} \bar{\boldsymbol{f}}^R \\ \bar{\boldsymbol{q}}^R \end{Bmatrix}, \quad (52)$$

where $\bar{\boldsymbol{K}} = \boldsymbol{T}^{m\mathrm{T}}\boldsymbol{K}\boldsymbol{T}^m$, $\bar{\boldsymbol{G}} = \boldsymbol{T}^{m\mathrm{T}}\boldsymbol{G}\boldsymbol{T}^n$, overbars correspond to the symmetry-adapted systems.

7 Implementation of partitioning algorithm

Use a complete symmetrized orthogonal basis adopted in Ref. [13], i.e.

$$\begin{aligned} &\boldsymbol{e}_1 = \{1, 1, \ldots, 1\}^{\mathrm{T}}/\sqrt{N}, \\ &\boldsymbol{e}_{2i} = \sqrt{2/N}\{\cos i\theta_1, \cos i\theta_2, \ldots, \cos i\theta_N\}^{\mathrm{T}}, \\ &\boldsymbol{e}_{2i+1} = \sqrt{2/N}\{\sin i\theta_1, \sin i\theta_2, \ldots, \sin i\theta_N\}^{\mathrm{T}}, \\ &\qquad i = 1, \ldots, [(N-1)/2], \\ &\theta_k = (k-1)\theta, \quad k = 1, 2, \ldots, N, \\ &\boldsymbol{e}_N = (1, -1, 1, \ldots, -1)^{\mathrm{T}}/\sqrt{N}, \quad \text{when } N \text{ is even}, \end{aligned} \quad (53)$$

where $[(N-1)/2]$ is the largest integer which does not exceed $(N-1)/2$. $\bar{\boldsymbol{u}}^R$, $\bar{\boldsymbol{\lambda}}^R$ can be expended as

$$\bar{\boldsymbol{u}}^R = \boldsymbol{E}^m\underline{\boldsymbol{u}}^R, \quad (54)$$

$$\bar{\boldsymbol{\lambda}}^R = \boldsymbol{E}^n\underline{\boldsymbol{\lambda}}^R, \quad (55)$$

$$\boldsymbol{E}^m = [\boldsymbol{e}_{rs} \cdot \boldsymbol{I}^m]^{\mathrm{T}}, \quad (56)$$

$$\boldsymbol{E}^n = [\boldsymbol{e}_{rs} \cdot \boldsymbol{I}^n]^{\mathrm{T}}, \quad (57)$$

where $\boldsymbol{I}^m$ and $\boldsymbol{I}^n$ are unit matrices of $2m$ and $2n$-dimensions, respectively. $\boldsymbol{e}_{rs}$ is the s-th element of the basis $\boldsymbol{e}_r$. Substituting Eqs. (54)–(55) into Eq. (52), we obtain

$$\begin{bmatrix} \underline{\boldsymbol{K}} & \underline{\boldsymbol{G}} \\ \underline{\boldsymbol{G}}^{\mathrm{T}} & \boldsymbol{0} \end{bmatrix} \begin{Bmatrix} \underline{\boldsymbol{u}}^R \\ \underline{\boldsymbol{\lambda}}^R \end{Bmatrix} = \begin{Bmatrix} \underline{\boldsymbol{f}}^R \\ \underline{\boldsymbol{q}}^R \end{Bmatrix}, \quad (58)$$

where $\underline{\boldsymbol{K}} = \boldsymbol{E}^{m\mathrm{T}}\bar{\boldsymbol{K}}\boldsymbol{E}^m$, $\underline{\boldsymbol{G}} = \boldsymbol{E}^{m\mathrm{T}}\bar{\boldsymbol{G}}\boldsymbol{E}^n$, $\underline{\boldsymbol{f}}^R = \boldsymbol{E}^{m\mathrm{T}}\bar{\boldsymbol{f}}^R$, $\underline{\boldsymbol{q}}^R = \boldsymbol{E}^{n\mathrm{T}}\bar{\boldsymbol{q}}^R$. It can be proved that $\underline{\boldsymbol{K}}$ and $\underline{\boldsymbol{G}}$ are block-diagonal and have the form

$$\underline{\boldsymbol{K}} = \sum_{m=0}^{[N/2]} \oplus \underline{\boldsymbol{K}}_{mm}, \quad (59)$$

$$\underline{\boldsymbol{G}} = \sum_{m=0}^{[N/2]} \oplus \underline{\boldsymbol{G}}_{mm}, \quad (60)$$

where $\oplus$ represents the direct sum of matrices. $\underline{\boldsymbol{K}}_{mm}$, $\underline{\boldsymbol{G}}_{mm}$ represent sub-matrices of $\underline{\boldsymbol{K}}$, $\underline{\boldsymbol{G}}$, respectively. For further detailed description of Eqs.(59)–(60), please refer to Refs. [19, 20].

Based on Eqs. (59)–(60), it is obvious that the solution problem of Eq. (58) can be naturally partitioned into $[(N+2)/2]$ decoupled subproblems,

$$\begin{bmatrix} \underline{\boldsymbol{K}}_{mm} & \underline{\boldsymbol{G}}_{mm} \\ \underline{\boldsymbol{G}}_{mm}^{\mathrm{T}} & \boldsymbol{0} \end{bmatrix} \begin{Bmatrix} \underline{\boldsymbol{u}}_m^R \\ \underline{\boldsymbol{\lambda}}_m^R \end{Bmatrix} = \begin{Bmatrix} \underline{\boldsymbol{f}}_m^R \\ \underline{\boldsymbol{q}}_m^R \end{Bmatrix}, \quad (m = 0, 1, \ldots, [N/2]), \quad (61)$$

where

$$\begin{aligned} &\underline{\boldsymbol{u}}_0^R = \underline{\boldsymbol{u}}^{1R}; \quad \underline{\boldsymbol{u}}_{N/2}^R = \underline{\boldsymbol{u}}^{NR} \quad (\text{when } N \text{ is even}), \\ &\underline{\boldsymbol{u}}_m^{R\mathrm{T}} = \{\underline{\boldsymbol{u}}^{pR\mathrm{T}}, \underline{\boldsymbol{u}}^{qR\mathrm{T}}\} \\ &(p = 2m, q = 2m+1; m = 1, 2, \ldots, [(N-1)/2]). \end{aligned} \quad (62)$$

Therefore, instead of solving the original system Eq. (30), now one needs only to solve a series of independent small subproblems as given by Eq. (61). Obviously, the partitioning of the original problem into a series of small subproblems will lead to a higher efficiency of computation, which will also be demonstrated by the numerical example given in the next section.

All discussed above is under arbitrary traction conditions; now consider a specific traction case (Fig. 2) where the load distributions have the same rotationally periodic symmetry as the structures, i.e.

$$\bar{\boldsymbol{f}}^{1R} = \bar{\boldsymbol{f}}^{2R} = \cdots = \bar{\boldsymbol{f}}^{NR}. \quad (63)$$

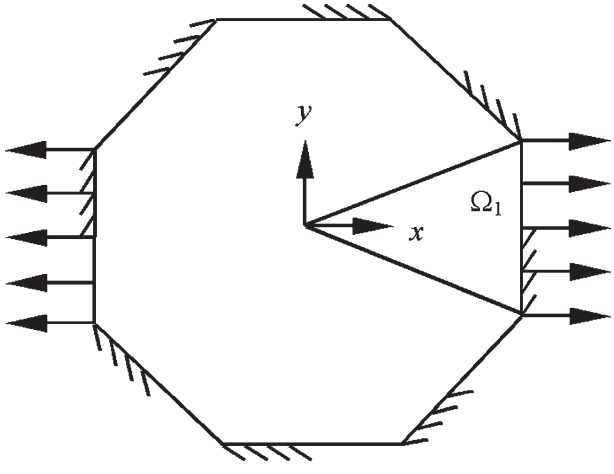

Fig. 2 A regular octagon plate subjected to tension along two opposite edges

Equation (63) leads to

$$\underline{f}^{2R} = \underline{f}^{3R} = \cdots = \underline{f}^{NR} = \mathbf{0}, \qquad \underline{f}^{1R} = \sqrt{N}\bar{f}^{1R}. \quad (64)$$

In the case of symmetric constraints, one has

$$\underline{q}^{2R} = \underline{q}^{3R} = \cdots = \underline{q}^{NR} = \mathbf{0}, \qquad \underline{q}^{1R} = \sqrt{N}\bar{q}^{1R}. \quad (65)$$

In the case where Eqs. (64) and (65) are satisfied, one needs only to solve the first subproblem, the other $[N/2]$ subproblems have zero solutions.

8 Numerical examples

In this paper, a cubic spline weight function [18] was used in the EFG analysis with a scaling parameter $d_{\max} = 3.0$.

Numerical Example 1

Consider a regular octagon viscoelastic plate subjected to uniform tension along two opposite edges, as shown in Fig. 3 where its geometry, physical properties and constraint conditions are invariant under $N = 8$ symmetry transformations. Plane stress condition was assumed with Young's Modulus $E = 10^6\,\mathrm{N/m^2}$ and Poisson ratio $\nu = 0.3$. The constitutive relationship can be described by Eq. (20) where $\tau_0 = 28\,\mathrm{d}$, $C(t,\tau) = \varphi(\tau)(1-\mathrm{e}^{-\gamma(t-\tau)}), \varphi(\tau) = (0.9+4.82/\tau)\times 10^{-5}$ and $\gamma = 3.0093 \times 10^{-7}\,\mathrm{s}^{-1}$.

The above problem is solved via the proposed algorithm with 440 nodes in the whole computational region, and compared with the solutions given by ANSYS Program with 921 nodes and 280 higher order (2D) eight-node elements. The EFG meshes were graded with additional refinement around the hinged-supports. A comparison of CPU times is shown in Table 1. A comparison is given for u_x at node B as shown in Fig. 3.

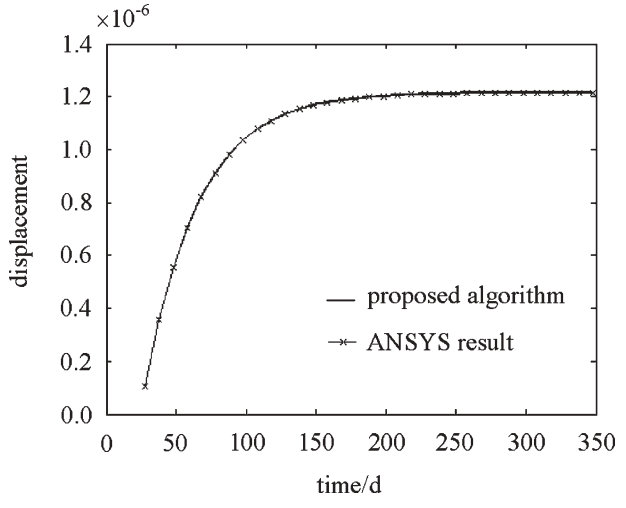

Fig. 3 Numerical comparison of u_x at node B ($x_{\mathrm{B}} = 0.66108$, $y_{\mathrm{B}} = 0.24314$)

Table 1 Comparison of CPU time

Solution method	80 nodes	120 nodes	168 nodes
Partitioning algorithm	45.094s	86.218s	153.578s
EFGM without partitioning	95.625s	215.766s	503.344s

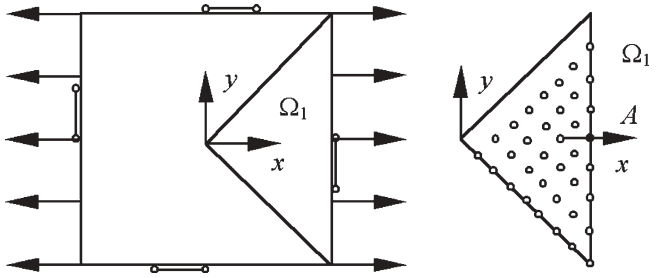

Fig. 4 A square plate subjected to uniform tension along two opposite edges ($x_{\mathrm{A}} = 0.5$, $y_{\mathrm{A}} = 0.0$)

Numerical Example 2

To compare the precision of the proposed method with analytical solutions, a square viscoelastic plate subjected to a uniform tension is examined as shown in Fig. 4(a) where $q = 1\,\mathrm{N}$, $N = 4$, $L = 1\,\mathrm{m}$, computing parameters are the same as those used in example 1. 144 nodes are used in the whole computational region. The mesh in the basic region is shown in Fig. 4(b) where the macula denotes node A. The comparison of u_x at node A is shown in Table 2. In Table 3, a solution of u_x given by the proposed algorithm with non-uniform sizes of time steps is compared with the analytical solution at node A.

Table 2 Comparison of u_x at Node A ($x_{\mathrm{A}} = 0.5$, $y_{\mathrm{A}} = 0.0$)

Days	Proposed algorithm/10^{-6}	Analytical solution/10^{-6}
28	0.5000	0.5000
48	2.6739	2.6737
68	3.9664	3.9659
88	4.7347	4.7342
108	5.1916	5.1910
128	5.4631	5.4626
148	5.6246	5.6240
168	5.7206	5.7200
188	5.7777	5.7770
208	5.8116	5.8110
228	5.8318	5.8311

Table 3 Numerical comparison of u_x at Node A with non-uniform sizes of time steps

t	β	Sizes of time step $u\big\|_{x=l}/10^{-6}$		Analytical solution/10^{-6}
31		3.0	0.9023	0.9022
34		3.0	1.2744	1.2743
64		6.0	3.7587	3.7583
70	0.000001	6.0	4.0624	4.0620
127		9.0	5.4527	5.4521
136		9.0	5.5379	5.5373
220		12.0	5.8249	5.8243

9 Conclusions

The major efforts of this paper are focused on improving computing accuracy in the time domain and saving computing expense at each discretized time interval. The major merits of this paper include:

(1) By using a two level expanding technique, a differential-integral equation system with boundary and initial values is converted into a series of recurrent linear boundary value problems. Self-adaptive computation can be carried out, providing a more precise description for the variation of variables, and compensating any possible loss of computing accuracy caused by improper choices of the size of time step.
(2) At each time step, by adopting a symmetry-adapted reference system, the coefficient matrices of EFG equation can be transformed into a block-circulant form, and then a partitioning algorithm was proposed, by which only series of small subproblems are required to be solved independently instead of the whole EFG equations under arbitrary load distributions. Thus the computational efficiency is significantly increased.

The overall approach presented, in terms of accuracy and efficiency, can be recommended as a useful tool for solving viscoelasticity problems.

References

1. Christensen, R.M.: Theory of viscoelasticity: an introduction. Academic Press. New York, 1982
2. Ouyang, H.: Fundamental theory of long term deformation in concrete and its application. Doctoral thesis, Dalian University of Technology, Dalian, China (1989)
3. Zeinkiewicz, O.C.: An implicit scheme for a finite element solution of problem of viscoplasticity and creep. C/R/252/75, University college of Swansea, UK (1975)
4. Zhu, B.: An implicity algorithom for analysis of creep stress in concrete structures. Chinese J Hydralic Eng **5**, 40–46 (1983)
5. Yang, H.T.: A precise algorithm in time domain to solve the problem of heat transfer. Num Heat Tran Part B **35**(2), 243–249 (1999)
6. Yang, H.T.: A new approach of time stepping for solving transfer problems. Communications in Num Meth in Eng **15**, 325–334 (1999)
7. Yang, H.T., Gao, Q., Guo, X.L., Wu, C.W.: A new algorithm of time stepping in the non-linear dynamic analysis. Commun in Num Meth in Eng **17**, 597–611 (2001)
8. Yang, H.T., Guo, X.L.: Perturbation boundary-finite element combined method for solving the linear creep problem. Inter J Solids and Struct **37**, 2167–2183 (2000)
9. Lu, Y.Y., Belytschko T., Tabbara M.: Element-free Galerkin method for wave propagation and dynamic fracture. Comp Meth in App Mech and Eng **162**, 131–153 (1995)
10. Thomas, D.L.: Dynamics of rotationally periodic structure. International Journal for Numerical Methods in Engineering, **14**, 81–102 (1979)
11. Williams, F.W.: Extract eigenvalue calculation for structures with rotationally periodic substructure. Inter J for Num Meth in Eng **23**, 695–706 (1986)
12. Wu, G.F., Williams, F.W., Kennedy, D.: Extract eigenvalue calculation for partially rotationally periodic structures. Comp and struc **64**, 275–284 (1997)
13. Wu, G.F., Yang, H.T.: The use of cyclic symmetry in two-dimensional elastic stress analysis by BEM'. Inter J solids and struct **31**, 279–290 (1994)
14. Zhong, W.X., Qiu, C.H., Cheng, G.D.: Some applications of group theory to the structure analysis. Acta Mechanica Sinica, **10**(4), 251–267 (1978) (in Chinese)
15. Qiu, C.H., Deng, K.S., Zhong, W.X.: Analysis of symmetric structures by multi-level substructuring and group-theoretic methods. Acta Mech Solida Sin **1**, 1–14 (1986)
16. Zienkiewicz, O.C., Morgan, K.: Finite Element and Approximation. New York: Wiley-Interscience Publication (1983)
17. Yang, H.T., Han, Z.: Solving non-linear viscoelastic problems via a self-adaptive precise algorithm in time domain. Inter J Solids and Struc **41**(20), 5483–5498 (2004)
18. Belytschko, T., Lu, Y.Y., Gu, L.: Element-free Galerkin methods. Inter J Num Meth in Eng **37**, 229–256 (1994)
19. Yang, H.T., Liu, L.: The use of cyclic symmetry in EFG analysis for heat transfer problems. Int J Numer Meth Engng **62**, 937–951 (2005)
20. Yang, H.T., Liu, L., Han, Z.: The use of cyclic symmetry in two-dimensional elastic analysis by the element-free Galerkin method, Commun Numer Meth Engng **21**, 83–95 (2005)